THE STRUCTURES OF THE MINERALS OF THE DESCLOIZITE AND ADELITE GROUPS: I—DESCLOIZITE AND CONICHALCITE (PART 1)

M. M. QURASHI[1] AND W. H. BARNES, *Division of Physics, National Research Council, Ottawa, Canada.*

ABSTRACT

Descloizite, Pb(Zn, Cu)(VO_4)(OH), and conichalcite, $CaCu(AsO_4)(OH)$, are typical members of the descloizite and adelite groups of minerals, respectively, and the determination of the structures of the individual members of both groups is dependent on the success with which that of descloizite can be established. The structure of descloizite has been found by a rigorously deductive and quantitative interpretation of Patterson maps. All important features have been brought out by preliminary Fourier syntheses; the atomic positions differ markedly from an arrangement recently proposed by Bachmann. The structure of conichalcite has been obtained by numerical comparison of Patterson maps with the corresponding ones for descloizite. Preliminary difference-syntheses have established the detailed similarity of the metal-atom positions in the two structures and have indicated some differences in the sites of the oxygen atoms. The oxygen coordination around the metalloid atoms (V, As) is approximately tetrahedral in both minerals.

INTRODUCTION

The minerals of the descloizite and adelite groups are very closely related in morphology and composition (Dana, 1951); they are orthorhombic with closely-similar axial lengths, and can theoretically be derived from one another by suitable substitution of appropriate metal atoms. The probable space group of descloizite, Pb(Zn, Cu)(VO_4)(OH), has been reported as *Pnma* (or *Pn2a*) (Bannister, 1933; Richmond, 1940; Barnes & Qurashi, 1952), while that of conichalcite, $CaCu(AsO_4)(OH)$, is $P2_12_12_1$ (Dana, 1951; Qurashi, Barnes & Berry, 1953). Hägele (1939) has argued from the resemblance of Weissenberg photographs of adelite, $CaMg(AsO_4)(OH)$, and descloizite that the space group of the latter is really $P2_12_12_1$, with the metal atoms in positions of *Pnma* symmetry, and that the effect of the deviations of the oxygen atoms from *Pnma* positions is masked by the heavy lead atoms. Conichalcite (Qurashi, Barnes & Berry, 1953) exhibits similar characteristics, viz., reflections contradicting the *n* and *a* glides of *Pnma* are all very weak, and some experimental evidence has also been obtained to support Hägele's contention regarding the space group of descloizite.

The present paper is the first of a series dealing with the structures of

[1] National Research Laboratories Postdoctorate Fellow, now with the Department of Scientific and Industrial Research, Government of Pakistan, Karachi.

the descloizite and adelite groups of minerals. It is limited to one representative of each, namely, descloizite and conichalcite. The structures of pyrobelonite, $MnPb(VO_4)(OH)$, (Strunz, 1939; Richmond, 1940; Barnes & Qurashi, 1952), and of the closely-related monoclinic mineral, brackebuschite, $(Mn, Fe)Pb_2(VO_4)_2 \cdot H_2O$ (Berry & Graham, 1948; Barnes & Qurashi, 1952), will be described in subsequent papers. The structural interest of these four minerals is evident from the precession photographs of the principal zones of each reproduced in Fig. 1 A, B. For direct comparison purposes, a *B*-centered cell ($B2_1/m$, or $B2_1$) for brackebuschite has been chosen and the orientation of the orthorhombic cells has been selected so that b coincides with the unique (b) axis of brackebuschite; this has the additional advantage of placing descloizite and pyrobelonite in the standard orientation (*Pnma; International Tables*, 1952) for D_{2h}^{16}.

Since the present investigation was commenced (Barnes & Qurashi, 1952), a structure for descloizite has been proposed by Bachmann (1953), based on Weissenberg data (Cu$K\alpha$ radiation), powder photographs (Cu$K\alpha$ radiation) and spectrometer records (Fe$K\alpha$, β and Cu$K\alpha$ radiation). Although atomic scattering factors and Lorentz-polarization factors were used in the structure factor calculations, there is no reference to absorption corrections which are significantly large with Cu, and especially with Fe, radiation. For various reasons, atomic positions and parameters, together with the coordinations of the oxygen atoms around the metal atoms, had to be assumed; it was not feasible to perform Patterson or Fourier analyses (Bachmann, private communication, 1953).

The solution of the structures of all minerals of the descloizite and adelite groups must depend ultimately on that for descloizite. For this reason the approach to the problem in this laboratory from the beginning has been as rigorously deductive as possible, and the interpretation of the experimental data is given in some detail in the present paper. This is particularly necessary in view of certain fundamental differences between the present structure and that obtained by Bachmann (1953).

In order to avoid any possible confusion throughout the present paper among references to Patterson projections, Fourier projections and structure projections, the first two are designated "maps" (with the appropriate adjective, Patterson or Fourier) and the term "projection" refers specifically to the structure. It is also convenient to denote "the (x, z) peak" in an ($h0l$) Patterson (or Fourier) map as "the (x, –, z) peak," the dash (–) indicating the undetermined coordinate; this convention has been adopted for the three principal zonal maps of each type.

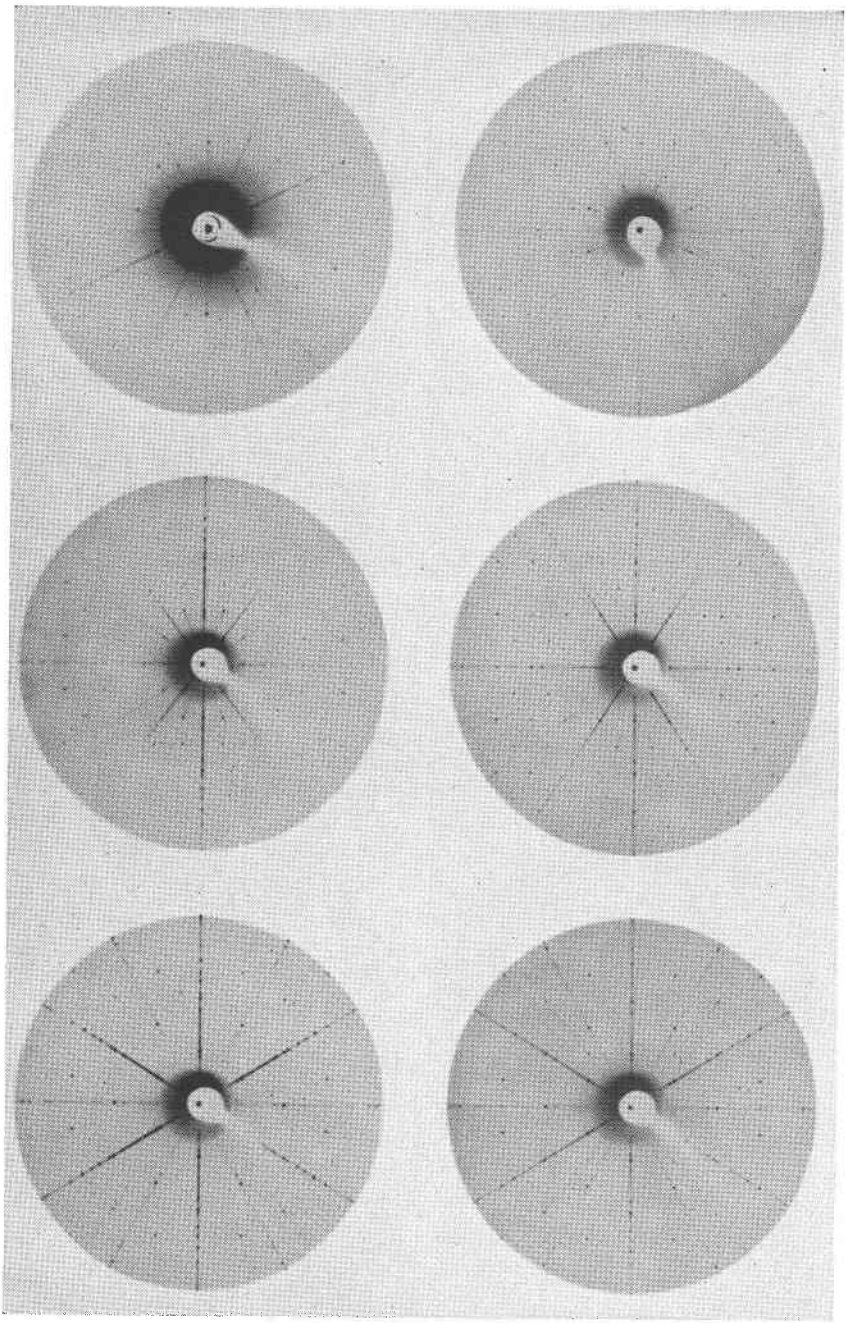

FIG. 1A. Zero level precession photographs ($\sim\frac{1}{2}$ scale) of (left hand column) brackebuschite, (right hand column) pyrobelonite; (top row) a^*c^* nets (a^* vertical); (middle row) b^*c^* nets (b^* vertical); (bottom row) a^*b^* nets (b^* vertical).

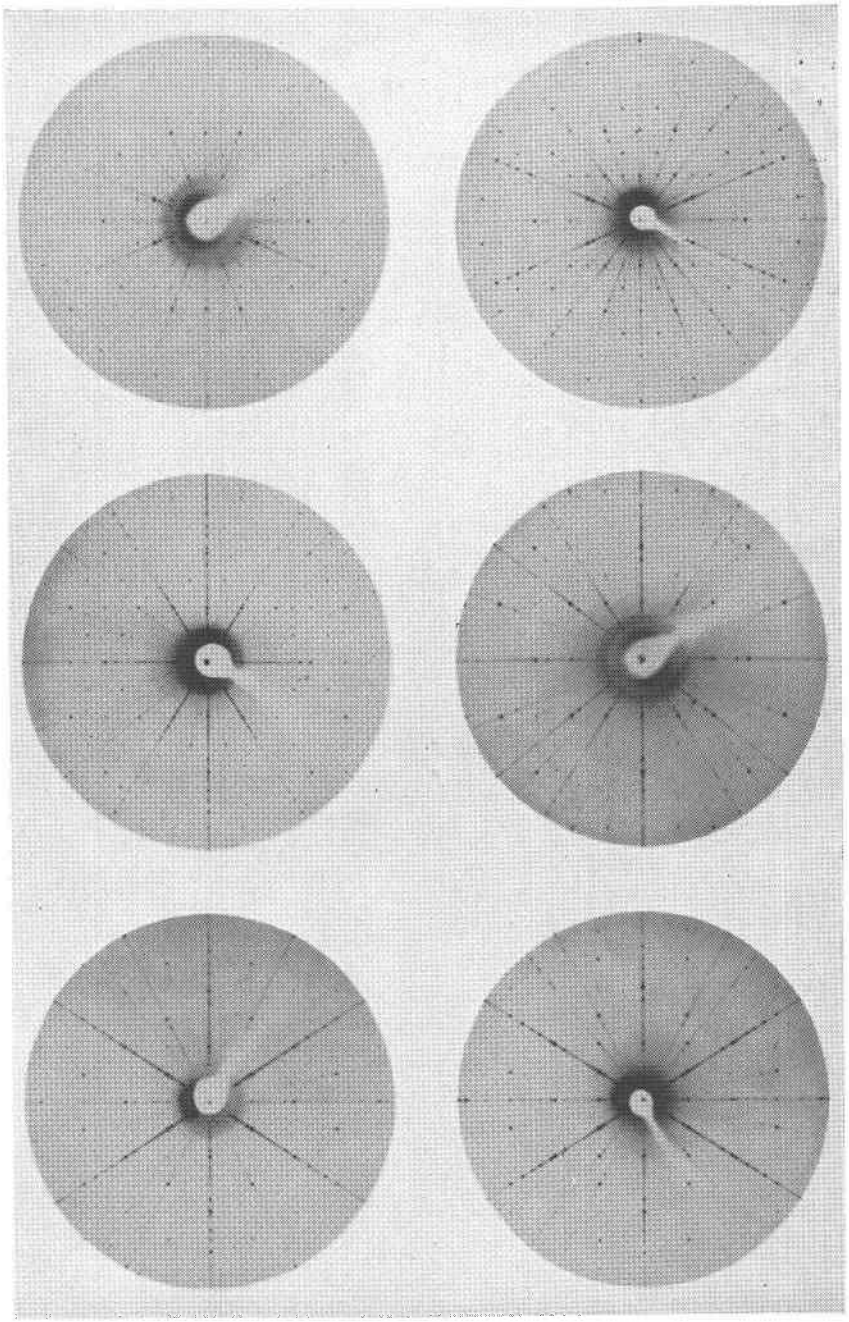

FIG. 1B. Zero level precession photographs ($\sim\frac{1}{2}$ scale) of (left hand column) descloizite, (right hand column) conichalcite; (top row) a^*c^* nets (a^* vertical); (middle row) b^*c^* nets (b^* vertical); (bottom row) a^*b^* nets (b^* vertical).

DESCLOIZITE

1. *Experimental*

The crystals of descloizite (Harvard Museum, 91040) from Los Lamentos, Chihuahua, Mexico, were kindly supplied by Professor Clifford Frondel. They were tabular {010} ({001} in *Pnam* orientation (Dana, 1951, p. 812)), and in many cases the observed faces were curved. The extinction was good and was used to align the crystals on the goniometer head to within $\pm 2°$. Some difficulty was experienced in obtaining a small equi-dimensional fragment of reasonably regular shape because the crystals have a conchoidal fracture and no cleavage. Two specimens of about 100 to 150μ, however, were finally obtained by careful cutting; it seemed impractical to use smaller ones. They were mounted with their *a* and *b* axes, respectively, parallel to the goniometer axis and Buerger precession photographs were obtained of the zero and upper levels along each of the three principal axes, using both filtered and unfiltered MoK radiation ($\lambda K\alpha = 0.7107$ Å) with $\bar{\mu} = 25°$. Zonal intensities were estimated visually from multiple exposures with a film-to-film ratio of 3.0 and an over-all exposure ratio of more than 200. They were corrected for the Lorentz-polarization factor by use of the revised calculations of Waser (1951), and for absorption by standard graphical methods. The upper level photographs were examined for absences and general intensity distribution. Intensity data also were obtained from 0*kl* Weissenberg films.

2. *Space group, and preliminary location of lead atoms*

The unit cell dimensions ($a = 7.60_7$, $b = 6.07_4$, $c = 9.44_6$ Å) and the space group (*Pnma*, or *Pn2a*) have been reported in an earlier paper (Barnes & Qurashi, 1952), together with a preliminary location of the lead atoms at $\frac{1}{8}, y, \frac{1}{6}$; $\frac{7}{8}, \frac{1}{2}+y, \frac{5}{6}$; $\frac{3}{8}, \frac{1}{2}+y, \frac{2}{3}$; $\frac{1}{8}, y, \frac{1}{3}$, with $y = \frac{1}{4}$ if the space group is *Pnma*. These coordinates were based on a general survey of *hkl* intensities and on preliminary Patterson maps. Thus, no violations of the systematic space group absences were observed on precession films after exposures of ten to twenty hours, from which it was inferred that at least the lead atom, and probably the zinc and vanadium atoms also, must be in *Pnma* (or *Pn2a*) positions.* The equivalent positions for *Pnma* are

(*a*) $0, 0, 0; 0, \frac{1}{2}, 0; \frac{1}{2}, 0, \frac{1}{2}; \frac{1}{2}, \frac{1}{2}, \frac{1}{2}$
(*b*) $0, 0, \frac{1}{2}; 0, \frac{1}{2}, \frac{1}{2}; \frac{1}{2}, 0, 0; \frac{1}{2}, \frac{1}{2}, 0$
(*c*) $x, \frac{1}{4}, z; \bar{x}, \frac{3}{4}, \bar{z}; \frac{1}{2}-x, \frac{3}{4}, \frac{1}{2}+z; \frac{1}{2}+x, \frac{1}{4}, \frac{1}{2}-z$
(*d*) $x, y, z; \frac{1}{2}+x, \frac{1}{2}-y, \frac{1}{2}-z; \bar{x}, \frac{1}{2}+y, \bar{z}; \frac{1}{2}-x, \bar{y}, \frac{1}{2}+z;$
$\bar{x}, \bar{y}, \bar{z}; \frac{1}{2}-x, \frac{1}{2}+y, \frac{1}{2}+z; x, \frac{1}{2}-y, z; \frac{1}{2}+x, y, \frac{1}{2}-z$

* In a 200-hour 0*kl* Weissenberg photograph, a few extremely weak reflections have been observed for which $k+l$ is odd (Qurashi, Barnes & Berry, 1953). Their effect on the

Of the $hk0$ reflections, those with $(h/2)+k$ odd are very weak while those with $(h/2)+k$ even are uniformly strong, thus suggesting that the Pb-Pb peaks in the ($hk0$) Patterson map should appear at $(\frac{1}{4}, \frac{1}{2}, -)$. Now, there are three sets of 4-fold and one set of 8-fold positions in *Pnma*, and these can each be described in terms of one or two sets of *Pn2a* positions (4-fold). With four lead atoms to place in the cell, the Pb-Pb peaks in the ($hk0$) Patterson map may be expected at $(2x_{Pb}, \frac{1}{2}, -)$, and thus $x_{Pb} \simeq \frac{1}{8}$. The choice of y_{Pb} is arbitrary in *Pn2a*, but in *Pnma*, since x_{Pb} is neither 0 nor $\frac{1}{2}$, the four lead atoms must be in position (c), and therefore $y_{Pb}=\frac{1}{4}$ (*International Tables*, 1952). (Even if the space group is *Pn2a*, y_{Pb} can still be taken as $\frac{1}{4}$ and the coordinates of the vanadium, zinc, and oxygen atoms can be fixed relative to this.) From the observation that the hkl intensities repeat after $l=6$, and that the strong reflections in the $\{h0l\}$ and $\{0kl\}$ zones vary approximately as $\cos 2\pi(l/6)$, it follows that $z_{Pb} \simeq \frac{1}{6}$.

These preliminary considerations indicated that no overlapping of lead atoms was to be expected in any of the principal projections, and that a detailed interpretation of Patterson maps should give definite information about the structure.

3. *Patterson maps*

In a structure of any complexity it is desirable to scale the Patterson maps carefully so that peak heights have a quantitative significance. This is particularly important in the case of decloizite if ambiguity between the positions of the vanadium and zinc atoms is to be avoided.

The intensities in each zone were first put on an absolute scale by Wilson's method (1942) of comparing $\bar{I}$ with $\sum_j f_j^2$ summed over all the atoms in the cell, a small estimated correction (10–20%) being introduced to allow for atoms overlapping in projection. The ratios of the three scale factors so obtained were then adjusted slightly on the basis of comparison with the ratios of the intensities of axial rows of reflections common to pairs of zones; in this way an averaged set of scale factors was obtained which was estimated to be correct to within about 10%.

The three Patterson maps, each for one-quarter of the cell, are shown in Fig. 2 with common edges adjacent to each other. The broken lines passing from one map to the next connect peaks that must correspond to the same interatomic vectors in both because they have one component in common. This device facilitates the three-dimensional location and interpretation of a particular interatomic vector. The correctness of

---

structure clearly will be very small and does not affect the present argument. They will be discussed in connection with the refinement of the structure.

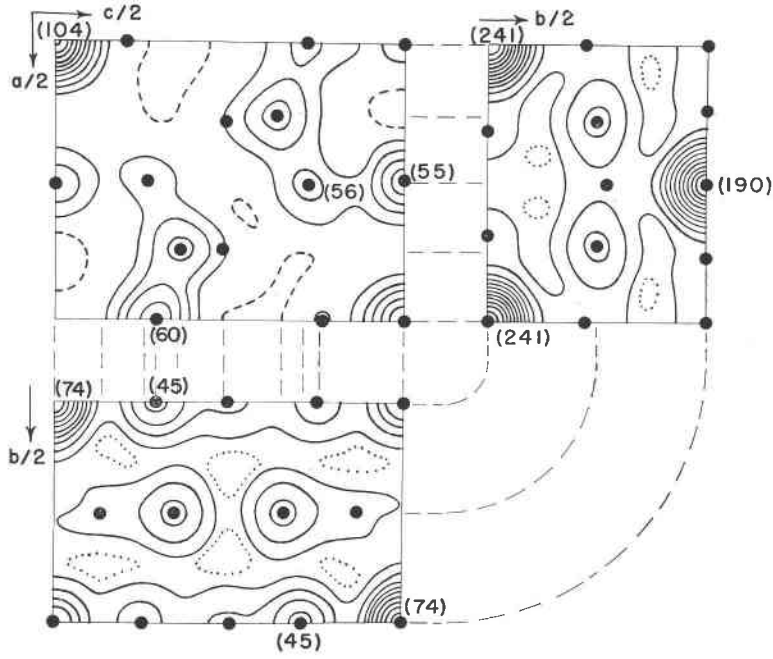

FIG. 2. Patterson maps for the three principal zones of descloizite, each over a quarter of the unit cell. Contours at intervals of 50 units with the 50-contour broken, and an extra contour at 75 units shown dotted in the ($hk0$) and ($0kl$) maps. The numbers in parentheses are the peak-heights remaining after subtraction of the Pb-Pb interactions.

the relative scales for the three maps is confirmed by the heights of the origin peaks; the slightly higher value for the $\{hk0\}$ zone is to be expected because of the appreciable depth of the cell (9.44 Å) and the consequent overlapping. From the values of these peak heights (after allowing for the effect of the lighter atoms), it can be estimated that a Pb-Pb peak of single weight, *i.e.*, one vector per unit cell, should have a height of about $450/4=112$. The height of a Pb-X peak of unit weight can then be estimated as follows. Place a Pb atom at (0, 0), an X atom at $(0, \frac{1}{2})$, and an X' atom at $(\frac{1}{2}, 0)$ in any given projection. It can then be shown, by calculating a theoretical Patterson map, that the peak heights, H, are related by

$$H(\text{Pb-Pb}):H(\text{Pb-}X):H(\text{Pb-}X') = \sum_{hk} f_{\text{Pb}}f_{\text{Pb}}:\sum_{hk} f_{\text{Pb}}f_X:\sum_{hk} f_{\text{Pb}}f_{X'}$$

where the products of the scattering factors, $f_{\text{Pb}}f_X$, etc., contain the temperature factor and the converging factor employed in the actual Patterson synthesis.* An approximation to the summations is obtained by an integral of the form

$$\int_0^{(\sin\theta_m)/\lambda} f_{Pb} f_X \frac{\sin\theta}{\lambda}\, d\left(\frac{\sin\theta}{\lambda}\right) \qquad (1)$$

where θ_m is the maximum value of the Bragg angle used for the Patterson synthesis. The integrals may be evaluated by calculating $f_{Pb}f_X$, etc., at 0.1 intervals of $\sin\theta/\lambda$ and then applying Simpson's rule. By this means the following values for the heights of peaks of unit weight were obtained:

Pb-Pb, 112; Pb-Zn, 37; Pb-V, 26; Pb-O, 8.5; Zn-Zn, 12.3; V-V, 6.2.

4. *The lead atoms*

On the basis of the preliminary survey of intensities, Pb-Pb peaks of weight 2 are to be expected at $(2x_{Pb}, \frac{1}{2}, -)$ and at $(\frac{1}{2}-2x_{Pb}, \frac{1}{2}, -)$ in the $(hk0)$ Patterson map. It is clear from Fig. 2 that only the observed peak of height 640 at $(\frac{1}{4}, \frac{1}{2}, -)$ can be interpreted as due to Pb-Pb, thus confirming $x_{Pb} = \pm\frac{1}{8}, \pm\frac{3}{8}$ (for the four equivalent positions). The quadruple weight is to be ascribed to overlapping of peaks $(2x_{Pb} \simeq \frac{1}{2}-2x_{Pb})$. Following the broken lines in Fig. 2 from the $(hk0)$ to the $(h0l)$ map, it is apparent that the Pb-Pb peaks in the latter must lie along $x=\frac{1}{4}, \frac{1}{2}$, the vectors being $(\frac{1}{2}\pm 2x_{Pb}, -, \frac{1}{2})$ of weight 2, $(2x_{Pb}, -, 2z_{Pb})$ of unit weight (unless $z_{Pb}=0$ or $\pm\frac{1}{4}$), and $\pm(\frac{1}{2}, -, \frac{1}{2}\pm 2z_{Pb})$ of weight 2 (unless $z_{Pb}=0$ or $\pm\frac{1}{4}$). Consideration of the $(\frac{1}{2}, -, \frac{1}{2})$ and $(\frac{1}{2}, -, \frac{1}{2}-\frac{1}{3})$ peaks along $x=\frac{1}{2}$ indicates that $z_{Pb}=0$ or $\pm\frac{1}{6}$, with equal probablility.

In the $(0kl)$ Patterson map, Pb-Pb peaks occur along $y=0$, at $(-, 0, \frac{1}{2}\pm 2z_{Pb})$ with weight 2 (unless $z_{Pb}=0$ or $\pm\frac{1}{4}$). Therefore, in Fig. 2 the only possible values of z_{Pb} are $0, \pm\frac{1}{6}$, the absence of a strong peak at $(\frac{1}{2}, -, 0)$ in the $(h0l)$ map ruling out $z_{Pb}=\pm\frac{1}{4}$. On this basis it follows that the lead atoms do not overlap in the $(0kl)$ projection, and, from the coordinates of special positions (*c*) (*Pnma, International Tables*, 1952), they cannot overlap in the $(hk0)$ projection owing to the operation of translational symmetry elements, thus establishing confidence in the estimate of 450/4 for a Pb-Pb peak of unit weight. Now, $z_{Pb}=0$ can be eliminated as a possible coordinate because the $(-, 0, \frac{1}{2})$ peak should have a weight of 4 and, consequently, a height of at least 450, whereas the observed value is only 288. Thus $z_{Pb} \simeq \pm\frac{1}{6}$ in agreement with the observed peak at $(-, 0, \frac{1}{2}-\frac{1}{3})$ of weight 2 and height 270, and with the earlier estimate based on a qualitative survey of the three-dimensional data.

The coordinates of the lead atom, therefore, are $(\frac{1}{8}, \pm\frac{1}{4}, \pm\frac{1}{6})$ to a sufficient approximation. Examination of the projections in Fig. 3 show that changing the signs of y_{Pb} and z_{Pb}, either singly or together, is merely

* Because the scattering factor of the Pb atom falls off rather slowly, an extra converging factor of $\exp(-4(\sin\theta/\lambda)^2)$ was used to damp out diffraction ripples caused by the termination of the series at $\sin\theta/\lambda \simeq 0.6$.

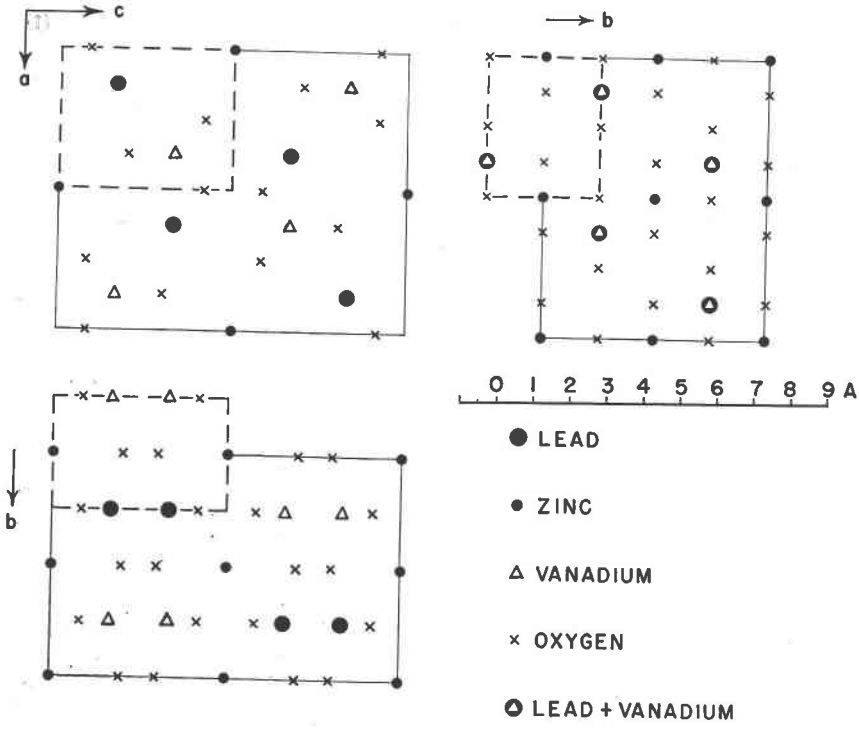

FIG. 3. Approximate structure of descloizite deduced from the Patterson maps.

equivalent to shifting the origin (from (0, 0, 0) to $(0, \frac{1}{2}, 0)$, $(0, 0, \frac{1}{4})$, or $(\frac{1}{2}, \frac{1}{2}, \frac{1}{2})$). The signs, therefore, can be taken arbitrarily as positive, and the positions of the lead atoms as $(\frac{1}{8}, \frac{1}{4}, \frac{1}{6})$, etc., represented by the large solid circles in the projections of Fig. 3. It is noteworthy that these sites are somewhat analogous to those occupied by the bismuth atoms in pucherite ($BiVO_4$, *Pnca*, special positions (*c*), $z_{Bi} \simeq \frac{1}{9}$, $c = 12.02$ Å; Qurashi & Barnes, 1953).

5. *The zinc and vanadium atoms*

Having fixed the positions of the lead atoms, the Patterson contributions from the Pb-Pb interactions can be calculated and then subtracted from the observed Patterson peaks. The residual map should represent Pb-*X* interactions, with perhaps a few *X*-*X'* interactions, the latter being in general much the weaker of the two. The subtraction is readily performed with the estimate of 112 for a unit Pb-Pb peak, and the resultant *difference* peak heights are given (in parentheses) beside the Pb-Pb peaks in Fig. 2. The high residual value of the (*hk*0) origin peak, and that

of the one at $(\frac{1}{4}, \frac{1}{2}, -)$, suggests that a metal atom overlaps the lead atom in the $(hk0)$ projection; from the peak heights ($\sim$200) it may be either a vanadium or a zinc atom, allowing $\sim$30 for the background. (When estimating the heights of the Pb-metal peaks a reasonable allowance for background is approximately one-half of the average background, which consists largely of Pb-O and X-X' interactions.) Analogy with the pucherite structure (in which Bi and V atoms both occupy the same type of special positions and overlap in the $(hk0)$ projection; Qurashi & Barnes, 1953) favours V as the atom overlapping Pb in the $(hk0)$ projection of descloizite. In any case, however, the effective height of a Pb-X peak in the $(hk0)$ Patterson map is increased by a factor of about $(f_{\text{Pb}}+f_{\text{metal}})/f_{\text{Pb}} \simeq 1.30$ due to this overlap.

All Pb-X peaks in the $(hk0)$ Patterson map must have a weight of at least 4 so that the axial peaks correspond to a unit Pb-X peak of height $\sim\frac{1}{4}((135-35)/1.3)=19$, which is rather small for a Pb-metal peak. On the other hand, the peaks at $(\frac{1}{4}\pm\frac{1}{8}, \frac{1}{4}, -)$ correspond to a unit Pb-X peak of height $\sim\frac{1}{4}((215-35)/1.3)=35$, which is just right for a Pb-metal peak. This places four metal atoms along $y=0, \frac{1}{2}$ with $x=0, \frac{1}{2}$, or $\pm\frac{1}{4}$. It is clear from both the $(hk0)$ and $(0kl)$ Patterson maps that $y=0, \frac{1}{2}$, or $\pm\frac{1}{4}$ for *all* metal atoms in the structure, and it is of interest to note that this is the limitation imposed by the special positions (a), (b), (c) of *Pnma*.

In Fig. 2 the broken connecting lines from the $(hk0)$ map to the $(h0l)$ and $(0kl)$ maps, lead from the peaks at $(\frac{1}{4}\pm\frac{1}{8}, \frac{1}{4}, -)$ to those at $(\frac{1}{4}\pm\frac{1}{8}, -, \frac{1}{4}\pm\frac{1}{12})$ and $(-, \frac{1}{4}, \frac{1}{4}\pm\frac{1}{12})$, respectively. These almost certainly represent Pb-metal vectors because they are effectively the strongest peaks in the "difference Patterson" maps. If they are due to a single Pb-X vector, then, from the $(0kl)$ peaks, the atom X must have $y=0, \frac{1}{2}$ and $z=0, \frac{1}{2}$, the other possibilities of $z=\frac{1}{6}, \frac{1}{3}$, etc. being ruled out by the absence of an equivalent peak at $(-, \frac{1}{4}, 0)$. This allocation gives a unit Pb-X peak of height of $\sim\frac{1}{4}(220-27)=48$, which corresponds to a metal atom (probably Zn) together with overlap from some other vectors. From the corresponding $(hk0)$ and $(h0l)$ peaks, it has already been established that $x=0, \frac{1}{2}$, or $\pm\frac{1}{4}$. The absence of peaks of height 120 at $(\frac{1}{8}, -, \frac{1}{6})$ and $(\frac{3}{8}, -, \frac{1}{3})$, however, eliminates the possibility of $x=\pm\frac{1}{4}$, and also requires overlapping atoms in the $(h0l)$ projection. Thus the x, z coordinates of the atom X must be 0, $\frac{1}{2}$, and $\frac{1}{2}$, 0 which are special positions (b) of *Pnma*; the unacceptable sets $(\frac{1}{4}, \frac{1}{2}; \frac{3}{4}, 0)$ are not consistent with $P2_12_12_1$, *Pn2a*, or *Pnma*, although the y, z coordinates $(0, 0; \frac{1}{2}, 0; 0, \frac{1}{2}; \frac{1}{2}, \frac{1}{2})$ would be.

Consideration of the $(-, 0, \frac{1}{2})$ peak of height 288, and of its associated peaks in the other two maps, shows that if it is also a Pb-X peak, the

coordinates of the atom X in this case must be $(-, y_{Pb}, z_{Pb}+\frac{1}{2})$, etc., *i.e.*, $(-, \frac{1}{4}, \frac{1}{2}+\frac{1}{6})$, $(-, \frac{1}{4}, -\frac{1}{6})$, etc., and the unit peak height would be $\sim\frac{1}{8}(288-28)=32$, thus corresponding again to a Pb-metal peak. If this is correct, a Patterson peak of height $\sim 32\times 4=128$ should be present at about $(-, \frac{1}{2}, \pm\frac{1}{6})$, (with a symmetrical one at $(-, 0, \frac{1}{2}\pm\frac{1}{6})$), and there is a rather diffuse peak of height 180 at $(-, \frac{1}{2}, \frac{1}{8})$. That this is not an independent peak is apparent from an examination of the peaks in the $(hk0)$ and $(h0l)$ Patterson maps corresponding to the $(0kl)$ peaks of heights 180 and 288. These two sets must correspond to the $(0, 0, -)$, $(\frac{1}{2}, 0, -)$, and $(\frac{1}{4}, \frac{1}{2}, -)$ peaks in the $(hk0)$ "difference Patterson" map (and to no others); they are equivalent to a unit Pb-X peak of height ~ 25, which is just right for a Pb-V peak.

The identification of the $(-, 0, \frac{1}{4})$ peak of height 158 is the next problem. Its associated peaks in the $(h0l)$ Patterson map, however, are not clearly defined, owing partly to the proximity of strong peaks. If it is assumed to represent a Pb-X vector, the coordinates of the atom X are $(-, \frac{1}{4}, \frac{3}{4}\pm\frac{1}{6})$ and the unit peak height $\sim\frac{1}{4}(158-27)=33$, which suggests either two oxygen atoms or an atom of vanadium. This makes the identification of the metal atoms a little less certain. There are, however, only three possible positions from which to choose (see Fig. 3) because the $(h0l)$ Patterson peaks corresponding to the only remaining $(0kl)$ peaks (at $(-, \frac{1}{4}, \frac{1}{4}\pm\frac{1}{6})$) are barely detectable and therefore cannot be Pb-metal peaks.

The uncertainty can be resolved by the following device. In the $(0kl)$ projection place an "average" atom with $f=\frac{1}{3}(f_{Zn}+f_V+2f_O)$ in each of the three possible sites and calculate the structure factors using these "average" atoms together with the lead atoms; assume a centric projection which is valid for $P2_12_12_1$, $Pn2a$, or $Pnma$ because of the rational values of y. In this way enough signs should be established to construct a sufficiently good Fourier map for the identification of the doubtful atoms.

The signs of all but five of the $0kl$ reflections were fixed with reasonable certainty by this means and, of the five whose signs remained uncertain, three were too weak to be observed. The resulting $(0kl)$ Fourier synthesis, calculated with an artificial converging factor of $\exp(-3(\sin\theta/\lambda)^2)$ to reduce diffraction ripples, is plotted in Fig. 5. In order to interpret this Fourier map, theoretical estimates of the various peak-heights were obtained by placing a Pb atom at $y, z, = 0, 0$ and atoms X, X' at $y, z = 0, \frac{1}{2}$ and $\frac{1}{2}, 0$, respectively, in the $(0kl)$ projection. The Fourier peak heights are then equal to

$$8\pi \int_0^{(\sin\theta_m)/\lambda} f \frac{\sin\theta}{\lambda}\, d\left(\frac{\sin\theta}{\lambda}\right) \qquad (2)$$

(cf. equation (1)), where f includes any extra converging factor employed. In this way, the following peak-heights were deduced: Pb, 130; Zn, 43: V, 30; O, 9. On the basis of these values, it is apparent from the ($0kl$) Fourier map (Fig. 5) that the (–, 0, 0) position is occupied by an atom of zinc while that at (–, $-\frac{1}{4}$, $\frac{1}{6}$) is occupied by an atom of vanadium. In conjunction with the analysis of the Patterson maps, the coordinates of the Zn atoms, therefore, are now completely determined as ($\frac{1}{2}$, 0, 0), etc.

The information from the Fourier synthesis concerning the y, z, coordinates of the vanadium atoms can now be combined with the data from the Patterson maps to identify the (–, $\frac{1}{2}$, 0) and (–, $\frac{1}{2}$, $\frac{1}{8}$) Patterson peaks (heights 288 and 180, respectively) with Pb-V vectors. The corresponding ($hk0$) and ($h0l$) Patterson peaks enable ($x_{Pb}-x_V$) to be fixed as $\frac{1}{4}$, so $x_V=-\frac{1}{8}$. The coordinates of the V atoms, therefore, are ($-\frac{1}{8}$, $\frac{3}{4}$, $\frac{1}{6}$), etc.

Thus all the metal atoms are in special positions characteristic of *Pnma*, namely, Pb in (c) at ($\frac{1}{8}$, $\frac{1}{4}$, $\frac{1}{6}$), etc., V in (c) at ($-\frac{1}{8}$, $\frac{3}{4}$, $\frac{1}{6}$), etc., Zn in (b) at ($\frac{1}{2}$, 0, 0), etc., as shown in Fig. 3. This confirms one of Hägele's speculations regarding the structure of descloizite.

6. *The oxygen atoms*

Having established the positions of the metal atoms, the heights of the Pb-Pb, Pb-Zn, Pb-V, Zn-Zn, Zn-V, and V-V Patterson peaks can be calculated and then subtracted from the peak heights observed. In this way a set of "second difference Patterson" maps were obtained, the peaks of which should correspond largely to Pb-O, and in some cases to Zn-O and to V-O , interactions. These maps are shown schematically in Fig. 4; the small negative values for the ($hk0$) and the ($h0l$) origin peaks are due to insufficient allowance for overlapping when scaling the intensities.

Now from the ($0kl$) Fourier map (Fig. 5), it is apparent that one O atom must be situated in each of the approximate positions (–, 0, $\frac{1}{8}$) and (–, $-\frac{1}{4}$, $\frac{1}{12}$). It is highly probable that another O atom is present at $y=\frac{1}{4}$, $z\simeq\frac{1}{20}$, and that the (–, $-\frac{1}{4}$, $\frac{1}{12}$) Fourier peak is due to two overlapping atoms of oxygen (peak height, calculated, 18; observed, 15). This confirms the (–, 0, $\frac{1}{4}$) and (–, 0, $\frac{3}{8}$) peaks in the "second difference Patterson" maps (Fig. 4) as Pb-(2O) peaks (unit peak height $\sim 76/4=19$), and shows that the rather diffuse peak at about (–, $\frac{1}{4}$, $\frac{1}{12}$) (Figs. 2, 4) is composed of Pb-O and Zn-(2O) vectors (peak height, calculated, $\sim 32+20=52$; observed, 100). On the basis of the strong ($hk0$) peaks (Fig. 4), and the known y coordinates for these two pairs of O atoms, $x\simeq 1$, $\frac{1}{4}$, $\frac{1}{2}$, $\frac{3}{4}$ for the first pair (for which $y\simeq\pm\frac{1}{4}$) and $x\simeq\frac{1}{8}$, $\frac{3}{8}$, $\frac{5}{8}$, $\frac{7}{8}$ for the second pair (for which $y\simeq 1$, $\frac{1}{2}$). The extraordinary heights of the ($hk0$) peaks involved

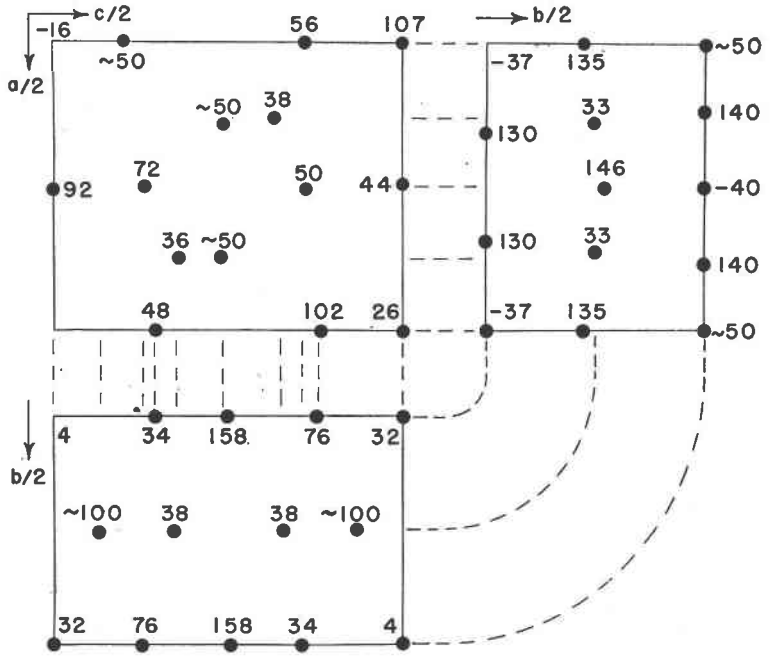

FIG. 4. Second difference Patterson maps obtained by subtracting all metal-metal peaks, thus leaving behind the metal-oxygen peaks plus the negligible oxygen-oxygen peaks.

(Fig. 4) are due to the fact that they represent overlaps of Zn-O and (Pb+V)-O vectors. Comparison with the observed ($h0l$) peaks (Fig. 4) now enables the z coordinates of the oxygen atoms to be obtained, bearing in mind that the zinc atoms overlap in the ($h0l$) projection (Fig. 3), and are therefore nearly as effective as the lead atoms.

The probable positions of most of the oxygen atoms were obtained in this way. The locations, of course, are somewhat uncertain, but ambiguities were largely removed with the aid of Fourier syntheses based on the signs obtained from the coordinates of the metal atoms. The approximate positions of the oxygen atoms are indicated by crosses in Fig. 3.

7. *Preliminary Fourier maps*

In section 5, the y and z coordinates of the zinc and vanadium atoms have been obtained directly from an ($0kl$) Fourier synthesis with signs determined by placing an "average" atom of scattering power $\frac{1}{3}(f_{Zn}+f_V+2f_O)$ in each of the three possible sites predicted by the Patterson maps. Since the present structure is significantly different from that proposed

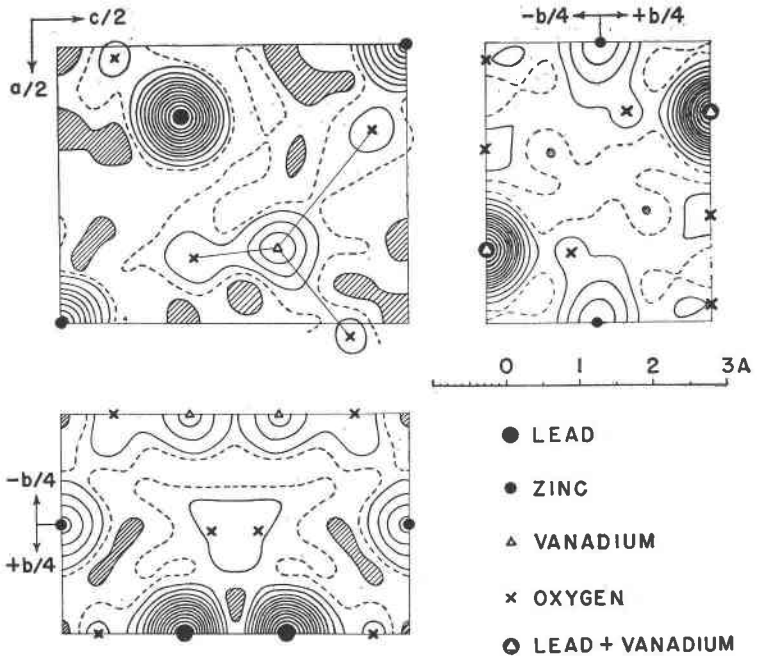

FIG. 5. Preliminary Fourier maps of the descloizite structure. Contours at intervals of 10 $e.Å^{-2}$; contour at 5 $e.Å^{-2}$ shown broken; negative regions hatched.

by Bachmann (1953), it is desirable to carry out a similar direct determination for the $\{h0l\}$ and $\{hk0\}$ zones.

From the argument presented in section 5, it is clear that the zinc, the vanadium, and two pairs of oxygen atoms must be located in the four different types of positions indicated in the $(h0l)$ projection (Fig. 3). The same device as that used for the $(0kl)$ projection (*i.e.*, placing an "average" atom in each of these positions) definitely fixed the signs of all but six of the observed reflections in the $\{h0l\}$ zone; the observed F's for these six reflections are between 20 and 40 as against 100 to 300 for the stronger reflections. The $(h0l)$ Fourier map, calculated with the signs obtained in this way, is shown in Fig. 5; it is remarkable for the fact that, in the regions of negative electron density, $-\rho$ nowhere exceeds $6e.Å^{-2}$. The map leaves little doubt about the essential validity of the previous locations for the zinc, the vanadium, and the two pairs of oxygen atoms. In particular, the absence of distortion in the contours around the peak at $(\frac{1}{2}, -, 0)$, together with the observed height of this peak $(81 = 2 \times 40.5)$, verifies the superposition of two zinc atoms required by special positions (b) of *Pmna*. Also, the probable overlapping of the two oxygen atoms at

$(-, -\frac{1}{4}, \frac{1}{12})$, etc. previously mentioned in connection with the $(0kl)$ Fourier map is now confirmed by the two peaks along $z \simeq \frac{1}{2} - \frac{1}{12}$). This also brings out the approximately tetrahedral coordination of oxygen atoms around the atoms of vanadium. The V-O distances are approximately 1.55 to 1.95 Å, and thus compare favourably with those in V_2O_5 (1.57 to 1.92 Å; Ketelaar, 1936; Byström, Wilhelmi & Brotzen, 1950) and in $BiVO_4$ (1.76 to 1.95 Å; Qurashi & Barnes, 1953). The oxygen configurations around the lead and zinc atoms also appear to be normal.

The signs of all but five of the structure factors observed in the $\{hk0\}$ zone were fixed by the same method; the observed values of these five are all less than 32. The resulting Fourier map also is shown in Fig. 5 and confirms the atomic coordinates already established.

It should be noted that in none of the Fourier maps of Fig. 5 are more than four resolved oxygen peaks observed in one-quarter of the cell. However, the coordinates of all five are readily inferred from the peak heights and by a combination of the information from all three maps.

Structure factors have been calculated with these coordinates, and the *R*-factors are 10%, 12%, and 15%, for the $\{hk0\}$, $\{0kl\}$, and $\{h0l\}$ zones, respectively, when the unobserved reflections are included. To obtain the parameters of the oxygen atoms with satisfactory accuracy, it is essential that the structure be refined by difference methods. This refinement will be discussed in a subsequent paper.

8. *Discussion of the structure proposed by H. Bachmann* (1953)

The principal projections of the structure of descloizite proposed by Bachmann (1953) are shown in Fig. 6. In order that these projections shall be directly comparable with those in Fig. 3, the *a*, *b*, and *c* axes of Bachmann (based on *Pmcn* adopted from Bannister, 1933) have been changed to *b*, *c*, and *a*, respectively, (*Pnma*), and the resulting *z* parameters (*y* in Bachmann's paper) have been altered by $\frac{1}{2}$.

It is obvious from Figs. 3 and 6 that, with the exception of the lead-atom positions, the two structures as a whole have nothing in common. On the other hand, individual projections do show certain similarities, and, with the exception of the vanadium in the $(h0l)$ projection, Bachmann has placed the atoms in the neighbourhood of one or other of the peaks of Fig. 5. His separation of the superposed zinc atoms in the $(h0l)$ projection can be attributed to the presence of the neighbouring (double) oxygen peaks. This separation displaces the four zinc atoms from the special positions (*b*) of *Pnma* into the general (8-fold) positions (*d*), unless the *y* coordinates are taken as $\pm\frac{1}{4}$ (instead of 0, $\frac{1}{2}$) to give the (4-fold) positions (*c*). This discrepancy of $\frac{1}{4}$ in the *y* coordinates of the zinc atoms is the basic difference between the structure (Fig. 3) deduced from

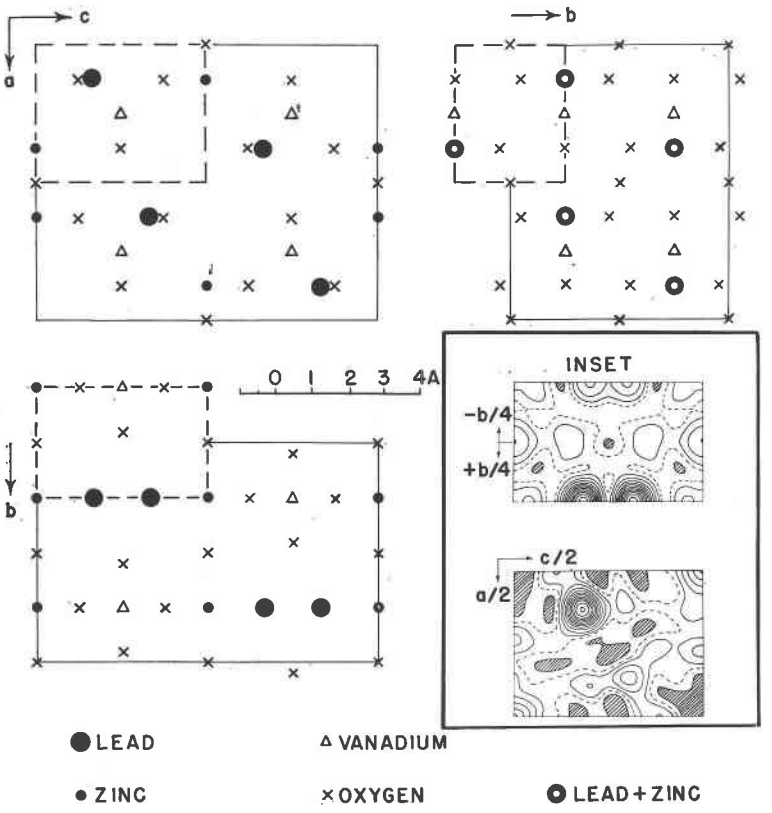

FIG. 6. Schematic representation of descloizite structure proposed by Bachmann; atoms designated as in Figs. 3, 5; note that Pb and Zn now overlap in the (*hk*0) projection. Inset: (0*kl*) and (*h*0*l*) Fourier maps obtained with magnitudes of the structure factors used in the present paper but signs fixed by Bachmann's structure; the similarity with Fig. 5 is apparent.

the Patterson maps, and that (Fig. 6) proposed by Bachmann; other differences, such as Bachmann's location of the vanadium atom in what is probably a diffraction ripple around the lead atom, can be ascribed to the use of assumed coordinations.

Finally, (*h*0*l*) and (0*kl*) Fourier maps, obtained by the use of only those structure factors whose signs are fixed definitely by the coordinates of Bachmann (*i.e.*, omitting terms for which $|F_c|$ is very small while $|F_o|$ may be large), are shown in Fig. 6) (inset). In spite of the conditioning effect of the signs, these maps correspond essentially to the structure of Figs. 3 and 5 rather than to that of Fig. 6.

Conichalcite

1. *Experimental and unit cell data*

The crystals of conichalcite (Harvard Museum, 92923), from the type locality, Bisbee, Arizona, also were kindly supplied by Professor Clifford Frondel. As in the case of descloizite, the lack of a cleavage, and the uneven fracture, made it difficult to obtain ideally shaped crystals for the structure investigation. Two fragments, however, about 150 μ in linear dimensions and approximately cubical, were cut and then mounted with their a and b axes, respectively, along the goniometer axis; a complete set of zero and upper level precession photographs were taken using both filtered and unfiltered MoK radiation. The intensities were estimated, corrected, and put on an absolute scale exactly as described for descloizite.

The dimensions of the unit cell are $a=7.40$, $b=9.21$, $c=5.84$ Å (Berry, 1951) and the space group is $P2_12_12_1$ (Qurashi, Barnes & Berry, 1953).

2. *Patterson maps*

Patterson maps covering a quarter of the cell for each of the three principal zones are plotted in Fig. 7; an extra converging factor of $\exp(-4(\sin\theta/\lambda)^2)$ was used for uniformity with descloizite. These maps bear a striking resemblance to the corresponding ones for descloizite (see Fig. 2); in fact, there is a peak-by-peak correspondence between them as far as the peak positions are concerned. This strongly suggests that the structure of conichalcite is approximately related to that of descloizite by appropriate replacement of Pb, Zn, and V atoms by atoms of Ca, Cu, and As, for which further support comes from a detailed examination of the heights of the various peaks. Also, the replacement of vanadium by arsenic, and of lead and zinc by calcium and copper, makes the $(0kl)$ Fourier map almost exactly symmetrical about $y=\frac{1}{2}$ and $z=\frac{1}{2}$, this feature being apparent even from inspection of the $0kl$ precession photographs (Fig. 1B) in which reflections with either k or l odd are very weak. Thus the $(0kl)$ Patterson map (Fig. 7) appears approximately symmetrical about $y=\frac{1}{4}$ and $z=\frac{1}{4}$. Finally, a number of peaks that are incipient or not observable in the descloizite Patterson maps emerge fairly clearly in those of conichalcite because of the lower scattering power of the heavy atoms in conichalcite which decreases their masking effect. Typical examples are the $(0, \frac{1}{2}, -)$ Patterson peak and the $(h0l)$ Patterson peaks corresponding to the $(0kl)$ peak at $(-, \frac{1}{4}, \frac{1}{7})$.

The interpretation of the Patterson maps for conichalcite, therefore, is essentially the same as for descloizite, providing the effect of the few very weak reflections that contradict the n and a glides of $Pnma$ (Qurashi,

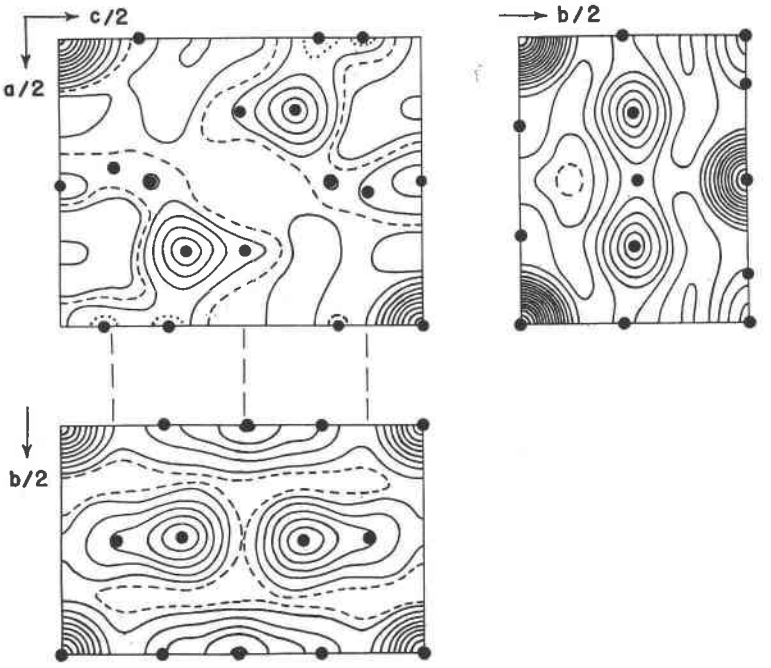

FIG. 7. Patterson maps for the three principal zones of conichalcite, each over a quarter of the unit cell. Contours at intervals of 10 units with the 45-contour broken, and sections of the 55-contour shown dotted.

Barnes & Berry, 1953) is ignored. This is justifiable because the effect will merely be to move some of the atoms slightly from the positions demanded by *Pnma* (or *Pn2a*) symmetry and it can best be taken into account during final refinement of the parameters. The problem, however, arises as to whether the lead atoms in the descloizite structure are replaced by the calcium atoms or by the copper atoms in conichalcite. The answer is not readily obtained from the Patterson maps. One solution would be to place an "average" atom with $f=\frac{1}{2}(f_{Ca}+f_{Cu})$ in each of the two possible positions (*i.e.*, those occupied by lead and zinc in descloizite), to calculate the signs of the structure factors, and then to identify the atoms from the Fourier peak heights. A better method is to plot difference syntheses, which will give directly the excess or deficit of the actual peak heights over the assumed values.

3. *Partial difference syntheses*

Since it was anticipated that the oxygen atoms in conichalcite might occupy different sites from those in descloizite, the signs for the first set

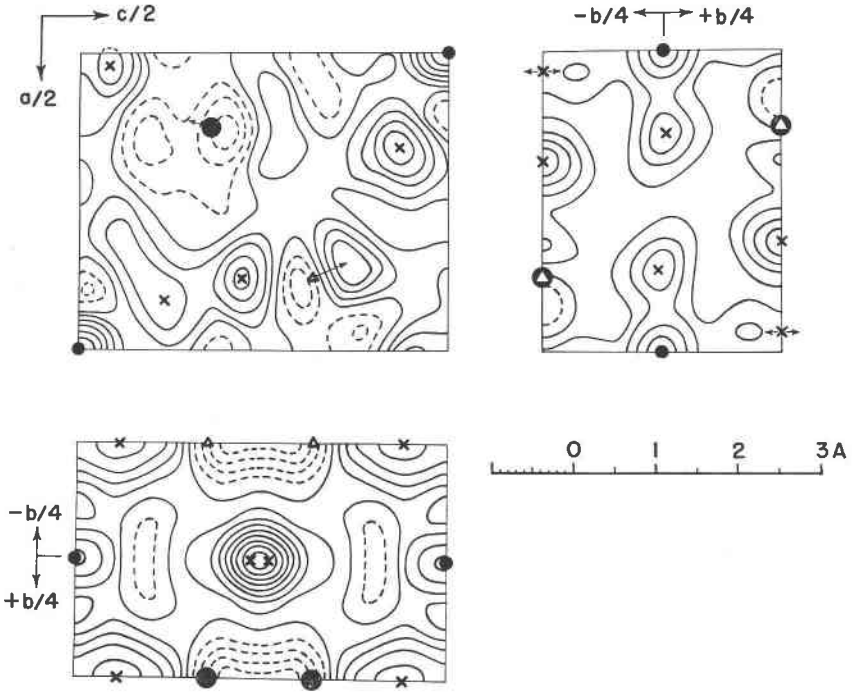

FIG. 8. Partial difference syntheses for conichalcite obtained by subtracting out the contributions of As and of $\frac{1}{2}$(Ca+Cu) placed in the possible positions for Ca and for Cu. Contours at intervals of 2 $e.Å^{-2}$ with the zero-contour and negative contours shown broken. Large solid circles, Ca; small solid circles, Cu; open triangles, As; crosses, O. The small arrows indicate the directions of some of the shifts.

of difference syntheses were calculated from the three metal atoms only, distributed as suggested in section 2. This procedure determined the signs of all but one of the observed reflections in the $\{hk0\}$ zone, and all but eleven of the observed reflections in the $\{h0l\}$ zone. For the $\{0kl\}$ zone, it was necessary to ignore all the terms with k odd because the calculated values are zero; the consequent error, however, is not large because, as mentioned previously, the observed F's for all such terms are small. The difference syntheses for the three zones are given in Fig. 8. Comparison with the Fourier maps of descloizite (Fig. 5) shows that the peaks corresponding to the zinc atoms are all positive (about $8e.Å^{-2}$ per zinc atom) from which it follows that copper replaces zinc. The peaks corresponding to lead atoms are negative in all three difference syntheses, although the effect in the ($hk0$) and ($0kl$) difference maps is diminished somewhat by effective overlapping with arsenic, and possibly by an

additional oxygen in the $\{hk0\}$ zone. The negative peaks, however, confirm that calcium (in conichalcite) must occupy the position of lead (in descloizite).

The three difference syntheses also give some information about the positions of the oxygen atoms. These are essentially the same as in the descloizite structure except that the two overlapping oxygen atoms along $x=\frac{3}{8}$ in the $(h0l)$ projection of descloizite (Figs. 3, 5) appear (Fig. 8) to have separated in conichalcite; this separation, however, turns out to be largely spurious on refinement of the structure. It is of interest that the $(hk0)$ difference map (Fig. 8) already gives indications of the shift of one oxygen atom away from special positions (c) of *Pnma* with $y=\pm\frac{1}{4}$.

The present R-factors for the conichalcite structure are 12%, 22%, and 22% for the $\{hk0\}$, $\{0kl\}$, and $\{h0l\}$ zones, respectively, when all the unobserved reflections are included. The refinement of the structure and the introduction of the weak reflections contradicting the *n* and *a* glides of *Pmna* will be considered at the same time as the refinement of the descloizite structure.

References

Bachmann, H. G. (1953): Die Kristallstruktur des Descloizit, *Acta Cryst.*, **6,** 102; Beiträge zur Kristallchemie natürlicher und künstlicher Schwermetallvanadate; II. Die Kristallstruktur des Descloizit, *N. Jahrb. Min.*, Mh., 9/10, 193–208.

Barnes, W. H., & Qurashi, M. M. (1952): Unit cell and space group data for certain vanadium minerals, *Am. Mineral.*, **37,** 407–422.

Bannister, F. A. (1933): The identity of mottramite and psittacinite with cupriferous descloizite, *Min. Mag.*, **23,** 376–386.

Berry, L. G. & Graham, A. R. (1948): *X*-ray measurements on brackebuschite and hematolite, *Am. Mineral.*, **33,** 489–495.

Byström, A., Wilhelmi, K. A. & Brotzen, O. (1950): Vanadium pentoxide—a compound with five-coordinated vanadium atoms, *Acta Chem. Scand.*, **4,** 1119–1130.

Dana, J. D. & E. S. (1951): *System of Mineralogy*, **2,** ed. 7, by C. Palache, H. Berman & C. Frondel, New York.

Hägele, G. (1939): Adelit und Descloizit, *N. Jahrb. Min.* Abt. A, Beil.-Bd. **75,** 101–109.

International Tables for X-Ray Crystallography (1952), Birmingham.

Ketelaar, J. A. A. (1936): Die Kristallstruktur des Vanadinpentoxyds, *Zeit. Krist.*, (A)**95,** 9–27.

Qurashi, M. M. & Barnes, W. H. (1953): The structure of pucherite, $BiVO_4$, *Am. Mineral.*, **38,** 489–500.

Qurashi, M. M., Barnes, W. H. & Berry, L. G. (1953): The space group of conichalcite, *Am. Mineral.*, **38,** 557–559.

Richmond, W. E. (1940): Crystal chemistry of the phosphates, arsenates, and vanadates of the type $A_2XO_4(Z)$, *Am. Mineral.*, **25,** 441–479.

Waser, J. (1951): The Lorentz factor for the Buerger precession method, *Rev. Sci. Instr.*, **22,** 563–566.

Wilson, A. J. C. (1942): Determination of absolute from relative *x*-ray intensity data, *Nature*, **150,** 152.